Preprints of the 21st IFAC World Congress (Virtual)
Berlin, Germany, July 12-17, 2020

Operator Performance Prediction based on Fuzzy Modeling Approach

Jianhua Zhang*, Zhong Yin**

*Dept. of Computer Science, Oslo Metropolitan University, 0166 Oslo, Norway (e-mail: jianhuaz@oslomet.no)
**School of Optical-Electrical and Computer Engineering, University of Shanghai for Science and Technology, Shanghai 200093, P. R. China (e-mail: yinzhong@usst.edu.cn)

Abstract: In this paper, physiological signals were measured from five participants, each participating in two sessions of experiment with identical experimental procedure. A simulation platform, AutoCAMS (Automation-enhanced Cabin Air Management System), was used to simulate a complex task environment of human-machine shared process control. Fuzzy models were constructed to quantitatively predict the human operator performance based on three EEG input features. The incremental-PID-controlled particle swarm optimization (IPID-PSO) algorithm was utilized to optimize the parameters of fuzzy models. The IPID-PSO algorithm incorporated incremental-PID-controlled search strategy to speed up the convergence of standard PSO algorithm. The operator performance modeling results are given to show the effectiveness of the IPID-PSO-tuned fuzzy modeling approach proposed to momentary operator performance assessment problem under consideration.

Keywords: Operator functional state; human performance; Human-machine systems; Physiological signals; EEG signals; Particle swarm optimization; PID control; Fuzzy modeling.

1. INTRODUCTION

Operator functional state (OFS) can be roughly defined as the temporally changeable ability of human operator to complete assigned cognition-demanding tasks. Since humans are good at making decisions and supervision, they are still involved, as an integral part (or agent), in many human-machine (HM) systems in such safety-critical fields as air traffic control, nuclear power industry and manned spaceflight. However, human operators cannot always be in good state due to the influence of mental effort, fatigue, anxiety, drowsiness, sleepiness, and other psychophysiological factors. To this end, an accurate OFS evaluation model is indispensably required to prevent potential human performance breakdown. Among various computational intelligence methods (Christensen, Estepp, Wilson and Russell, 2012), data-driven fuzzy system is highly suited to OFS estimation problem because of its transparency of structural knowledge representation, human-like inference mechanism, universal function approximation ability, and tolerance of fuzziness and other types of uncertainties in data (Lin, Ko, Chuang, Su and Lin, 2012).

It has been demonstrated in a variety of literature that OFS can be measured indirectly by physiological features, such as EEG spectral power (Gundel and Wilson, 1992), ECG features including heart rate and heart rate variability (HRV) (Bousefsaf, Maaoui and Pruski, 2013; Guerrero, Spinelli and Haberman, 2016), EOG features including blink interval, duration and frequency (Fairclough, Venables and Tattersall, 2005), blood pressure, respiratory activity, and others. Adaptive support vector machines (SVM) were used to classify mental workload (MWL) of six participants in Zhang, Yin and Wang (2015). In our work, support vector classifiers can precisely classify the measured physiological data into three or four levels at each time instant. In Wang, Zhang, Zhang and Wang (2012), the authors used three EEG features and one ECG feature as the inputs of OFS fuzzy model and achieved good modeling accuracy. The authors used adaptive-network-based fuzzy inference system (ANFIS) which was optimized by intelligent optimization algorithm of differential evolution (DE). Lin and Lin *et al*. (2012) employed a self-organizing neural fuzzy inference network (SONFIN) to model the OFS which was quantified by the reaction time of driver and a high modeling accuracy (i.e., the RMSE was 0.076) was obtained.

This paper develops a new particle velocity updating strategy. By integrating the incremental PID-controlled search mechanism into the standard particle swarm optimization (PSO) algorithm, a new PSO variant, called IPID-PSO, is proposed. The analysis of particle trajectory in PSO algorithm is transformed to performance analysis of a PID control system. Furthermore, in order to alleviate the performance degradation due to premature convergence, a mutation operator is adopted in the proposed IPID-PSO algorithm. The mutation takes place on both each particle and their best memories ***Pbest***. The IPID-PSO algorithm is used to identify fuzzy rule base for fuzzy model based human operator performance prediction.

2. DATA MEASUREMENT AND PREPROCESSING

The physiological and operator performance data collection experiments and data preprocessing approaches are described in this Section.

2.1 Experimental Equipment and Tasks

The AutoCAMS software (Bleil and Manzey, 2008) was used in the experiments to simulate human-machine shared

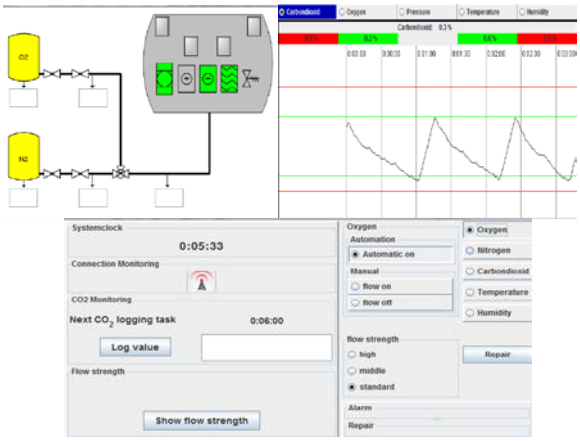

Fig. 1. The AutoCAMS simulation software: Schematic of system configuration and GUI (upper) and control panel (lower).

process control task environment. Fig. 1 shows the interface of AutoCAMS software. The cabin air quality indices include CO_2 concentration, O_2 concentration, air pressure and temperature, each of which is controlled by a separate control system. Each of the four subsystems has two modes of operation, manual control and automatic control. When certain faults occur in a subsystem, manual control mode must be initiated to permit the operator to open or shut down some switches on the control panel to maintain the safety of the subsystem. In mode of fault-free automatic control, control of the subsystem is automatically performed by computer. The operator monitored the time responses of the controlled variables and decided whether or not the O_2 valve, N_2 valve, CO_2 switch or heater switch should be opened or closed to make sure that the controlled variables are in normal range (green line in Fig. 1b). The detail descriptions of AutoCAMS functionalities can be found in our previous work [7].

2.2 Experimental Participants

Five participants (21-24 years old; coded by M, N, R, S and U) were selected to participate in our experiments. They all were male, healthy, right-handed, postgraduate students with normal or correct-to-normal vision from East China University of Science and Technology, Shanghai. Prior to formal sessions of experiment, each participant had been informed of the experimental aims and procedures so that he can better participate in the sessions. Furthermore, each participant received a training program on the AutoCAMS operations for over two hours so that he became familiarized with the software and manual control tasks skilfully.

2.3 Data Recording

Each participant took part in 2 sessions of experiments and each session consisted of 6 control task-load conditions with different levels of task difficulty. In different conditions, the participant was required to manually control a different number of subsystems in their target (or normal) ranges in collaboration with automated systems in AutoCAMS, i.e., in each session the number of manually controlled subsystems

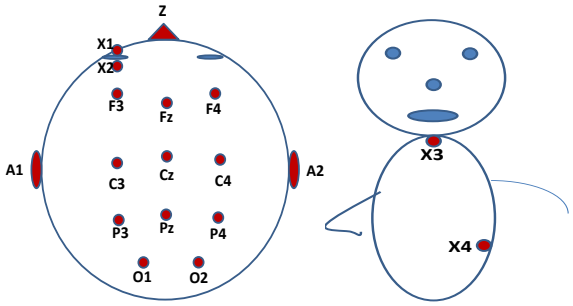

Fig. 2. The physiological signal measurement electrodes used.

in 6 conditions was 1, 3, 4, 4, 3 and 1, respectively. Each session lasted 90 m (=6 conditions *15 m per condition).

Using Nihon Kohden EEG device (made in Japan) which is able to automatically filter out the 50 Hz power line interference, the psychophysiological data were recorded with a sampling rate of 500 Hz. The electrophysiological signals, including EEG, EOG and ECG, were collected by placing 18 electrodes (i.e., F3, F4, Fz, C3, C4, Cz, P3, P4, Pz, O1, O2, X1, X2, X3, X4, A1, A2 and Z) on different regions of scalp or human body.

Fig. 2 shows schematically the locations of the 18 measurement electrodes used, in which X1 was placed under the eye, X2 above the eye, X3 on the bottom of neck and X4 on the waist were used to measure the ECG signal, Z on nasion used to replace the grounding electrode, and C3, C4, A1 and A2 (both placed on the left and right earlobes) used to measure the electrode resistance. For EEG measurement, 11 electrodes (i.e., F3, F4, Fz, C3, C4, Cz, P3, P4, Pz, O1 and O2) in international 10-20 system were placed on the scalp of the participant.

2.4 Data Preprocessing

The raw electrophysiological data measured was preprocessed for subsequent modeling and analysis. This Section introduces the approaches to preprocessing subjective evaluation data, raw EEG data (measured with a sampling rate of 500 Hz) and performance data (measured with a sampling rate of 1 Hz).

1) EEG data

The EOG artifacts were eliminated from raw EEG data by using FastICA algorithm (Shang, Huang, Du and Zheng, 2006). Then the EEG signal was filtered by a band-pass filter with the passing frequency band 0.5-40 Hz.

2) Performance data

The OFS was quantified by operator performance index, time in range (*TIR*), which was thus regarded as the model output and calculated by:

$$TIR = \frac{T'}{T} \times 100\% \quad (1)$$

Table 1. EEG input features for the OFS model of each participant.

Participant	M	N	R	S	U
Model inputs	*Fz*-θ	*F3*-θ	*Fz*-θ	*F4*-θ	*Fz*-θ
	Pz-α	*Pz*-α	*Pz*-α	*C3*-α	*Pz*-α
	TLI_1	TLI_1	TLI_1	TLI_1	TLI_1

where T' is the number of manually controlled subsystems in the normal range and T is the total number of manually controlled subsystems. Here T=4.

2.5 Input Selection for OFS Model

To select effectively the input variables of OFS model, we calculated linear correlation coefficients of the preprocessed physiological and TIR time-series data. The correlation coefficient r is calculated by:

$$r = \frac{(X - \overline{X}) \cdot (Y - \overline{Y})}{\sqrt{(X - \overline{X})^2} \cdot \sqrt{(Y - \overline{Y})^2}} \tag{2}$$

Where X and Y are two time series column vectors, and $\overline{X}$ and $\overline{Y}$ are their mean values.

Due to this significant individual difference, different input variables should be selected for the individualized OFS model across five participants. Based on correlation analysis results, three input variables were selected for each participant as shown in Table 1.

The selected input variables mainly include frontal theta band power and parietal-occipital alpha band power, which were also widely used in literature (e.g., Zhang, Yin and Wang, 2015; Wang, Zhang, Zhang and Wang, 2012; Hart, 2006). The central C3 alpha was selected to be an input for the OFS model of participant S. The parietal Pz alpha power was selected by four participants, which indicated that it is a salient marker of OFS variations.

Furthermore, due to its negative correlation with TIR data (r=-0.5569, -0.3599, -0.2554, -0.6336, and -0.2664 for five participants respectively), the following ratio of the two EEG powers, called TLI_1 (Task Load Index 1) (Wang, Zhang, Zhang and Wang, 2012), was used as an additional input:

$$TLI_1 = \frac{P_{Fz-\theta}}{P_{Pz-\alpha}} \tag{3}$$

Where $P_{Fz\theta}$ denotes theta band power at Fz electrode and $P_{Pz\alpha}$ denotes alpha band power at Pz electrode.

3. INCREMENTAL PID CONTROLLED PSO ALGORITHM

In addition to the IPID-controlled search mechanism, several new strategies are integrated into standard algorithm to constitute a new PSO variant, called Incremental PID controlled PSO (IPID-PSO) algorithm (Zhang and Yang, 2014). The computational procedure of IPID-PSO algorithm consists of seven steps:

Step 1: Initialize the population $\boldsymbol{X}$, set the initial velocity of the particle $\boldsymbol{v}$, calculate the current error $\boldsymbol{e}$ between $\boldsymbol{X}$ and ***Pbest***, save the best particle as ***Gbest***, set T=7. The mutation probabilities are opp_1 and opp_2. The particle number $i = 1, 2, \cdots, PopSize$ and the dimension $d = 1, 2, \cdots, D$. Let t=1, i=1 and d=1.

Step 2: Calculate the error between current particle and its randomly-selected exemplar $e_{i,d}^t = Pbest_{r(i)} - x_{i,d}^t$, where $\boldsymbol{r}$ is a vector containing randomly sorted integers from 1 to *PopSize*. Then update particle. If d<D, repeat **Step 2** and let $d \rightarrow d$+1. Otherwise proceed to **Step 3**.

Step 3: Compare the particle's fitness value to $Pbest1_i^t$ and $Gbest^t$. Here $Pbest1$ is a temporary set which preserves better particles during the 7 iterations. If its fitness is better than that of $Pbest1_i^t$, then replace $Pbest1_i^{t+1}$ with x_i^{t+1}; if its fitness is better than that of $Gbest^t$, then replace $Gbest^{t+1}$ with x_i^{t+1}.

Step 4: Mutate x_i^{t+1}. If i<*Popsize*, loop back to **Step 2** and let d=1 and $i \rightarrow i$+1. Otherwise proceed to

Step 5: Mutate $Pbest^{t+1}$.

Step 6: If T=0, then regenerate the new learning target index vector $\boldsymbol{r}$ and let T=7 and **Pbest** = **Pbest**1; If T>0, then proceed to **Step 7**.

Step 7: If t<FE, then loop back to **Step 2** and let i=1, d=1, $T \rightarrow T$-1, and $t \rightarrow t$+1. Otherwise terminate the algorithm and output the final result **Gbest**.

4. FUZZY OFS MODELING BASED ON IPID-PSO ALGORITHM

Since fuzzy system was already shown mathematically to be an universal approximator, in this Section we employ IPID-PSO algorithm to estimate the parameters of fuzzy OFS model, which consist of rule-base parameters and I/O MF parameters.

4.1 IPID-PSO-Tuned Fuzzy Model

The key of using PSO algorithm to determine model structural parameters is concerned with how to code a fuzzy model with a particle. In terms of fuzzy model of OFS, we adopt Mamdani-type fuzzy system consisting of a set of fuzzy production rules of the following IF-Then form (Wei, Qiu, Shi and Chadli, 2017; Xiong, Yu, Lü and Yu, 2014; Mehran, Giaouris and Zahawi, 2010):

$$\begin{aligned} R^j: &\text{If } x_1 \text{ is } A_{1j} \text{ and } x_2 \text{ is } A_{2j}, \cdots, \text{and } x_n \text{ is } A_{nj}, \\ &\text{Then } y \text{ is } B_j,\ j = 1, 2, \cdots, K \end{aligned} \tag{4}$$

where A_{ij} is the fuzzy subset of input (linguistic) variable x_i in the j-th fuzzy rule, characterized by its Gaussian membership function (MF):

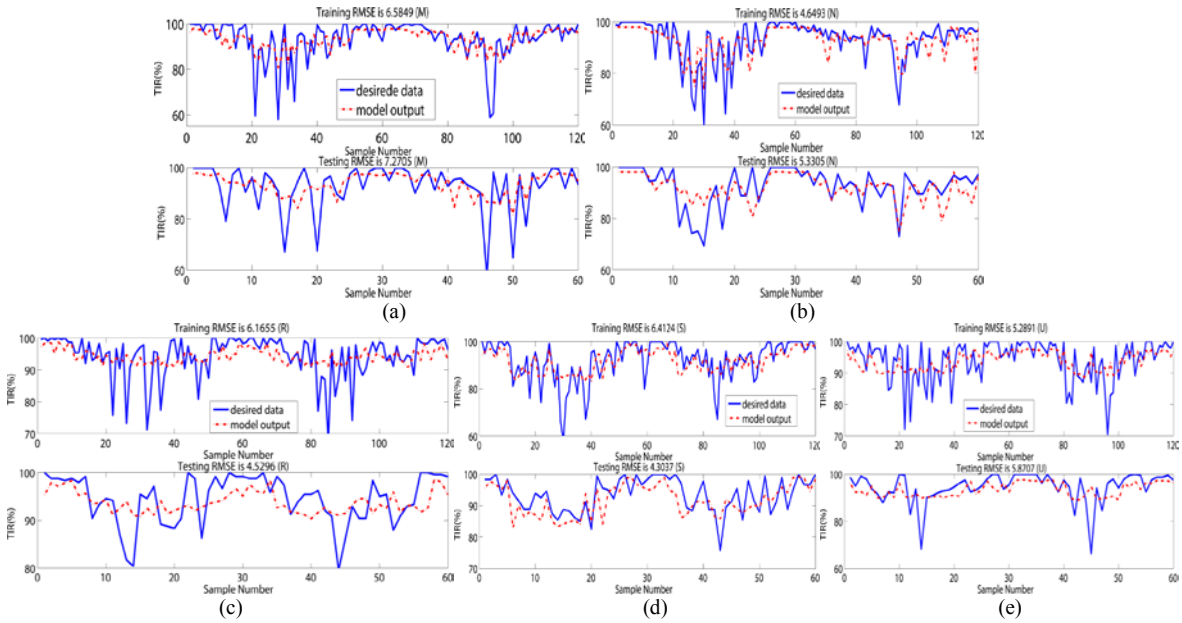

Fig. 3. The fuzzy model training and testing results: (a) M; (b) N; (c) R; (d) S; (e) U.

$$\mu_{A_{ij}}(x_i) = \exp[-\left(x_i - c_{ij}\right)^2 / (2\sigma_{ij}^2)] \tag{5}$$

with c_{ij} and σ_{ij} being the center and width parameters of the Gaussian MF, y is the output of fuzzy model, B_j is the output fuzzy subset, and K is the number of fuzzy rules in the rule base.

Using singleton fuzzification, product fuzzy reasoning and centroid (weighted average) defuzzifcation methods, the analytical formula of the crisp output of fuzzy model can be explicitly expressed by:

$$y = \frac{\sum_{j=1}^{K}\left[\prod_{i=1}^{n}\mu_{A_{ij}}(x_i)\cdot y_j\right]}{\sum_{j=1}^{K}\prod_{i=1}^{n}\mu_{A_{ij}}(x_i)} \tag{6}$$

where y_j denotes the core (or central value) of B_j.

Assume that each I/O variable is partitioned into m fuzzy subsets, each characterized by its Gaussian MF, then there are $2m(n+1)$ MF parameters to be optimized. The real-coding scheme is used to code each candidate fuzzy rule base, hence the length of rule-base segment in the particle is $K(n+1)$. When the particle is decoded, each bit on rule-base segment of the chromosome, a real number in the interval (0, 1), is multiplied by m, whose value is rounded upward to obtain the corresponding fuzzy subset in the rule.

The core of OFS estimation model is the fuzzy rule base, which is pre-defined as follows:

1) Let n=3, m=3 and K=16, i.e., each fuzzy model has three inputs and a single output, each I/O variable is partitioned into three fuzzy subsets (for convenience, specified by natural number 1, 2 and 3, respectively), and there are 16 fuzzy rules in the rule base.

2) Each Gaussian MF has two parameters, center c and width parameter σ.

Each particle codes the entire rule-base of a fuzzy model, i.e., 16 fuzzy rules and all parameters involved in each rule. When n=3, m=3, and K=16, each particle consists of two segments, rule-base and MF parameters and that each particle codes a fuzzy model. The length (number of bits) of each particle is 88 (=64+24=16×4+2×3×4). Each bit of this string is a real number in the interval (0, 1).

The objective function, to be minimized, is defined by the root mean squared error between the model output and measured *TIR*:

$$RMSE = \sqrt{\frac{1}{N}\sum_{i=1}^{N}(\hat{y}_i^{\,2} - y_i^{\,2})} \tag{7}$$

where $\hat{y}_i$ is the model output, y_i is the actual (or desired) output, and N is the number of sample data pairs.

4.2 Fuzzy modeling results

In this Section, the aforementioned four PSO variants are used to identify individualized fuzzy OFS model for each participant. First the measured data from two sessions were concatenated, then two thirds of the combined data were regularly extracted as the training set and the remaining one third of data used as the testing set. There were 10 simulation runs of each PSO variant, the swarm (population) size was set to be 30 and maximum number of iterations for each run was set to be 300. The model training RMSE was calculated for each run.

Fig. 3 presents the training and testing results of IPID-PSO-optimized fuzzy model for each participant. It is shown that

fuzzy OFS models identified by using the IPID-PSO algorithm can accurately estimate operator performance (i.e., *TIR*). In particular, for participant M, N, and S, the model output has more dynamics and thus not only fits well the measured TIR data, but detects successfully those risky state (with *TIR* declined under 80%). For participant R and U, the individualized model output seems flatter and thus captures the main trend of performance fluctuation but fails to detect the possibly risky or vulnerable state with sharp variation in operator performance.

On the other hand, for participant M, R and S, there is bigger difference between modeling training and testing accuracy. The training RMSE is smaller than the testing one for participant M, while it is larger in the case of participant R and S. This discrepancy between model training and testing accuracy may be due to the fact that there is session-to-session variability and unstationarity in physiological data for a participant and that the measured physiological data is indispensably noisy. Nevertheless, for participant N and U, the model achieves a better balance between training and testing (or generalization) performance possibly because the mental (or psychological) state and performance of the two well-trained participants is more stable in two sessions of experiment.

4.3 Analysis of Fuzzy Rule-based Models

As an example, Table 3 presents fuzzy rule base of fuzzy OFS model identified by IPID-PSO for participant N. The fuzzy partition of I/O domain is shown in Fig. 4, where the linguistic labels (or semantics) of fuzzy subsets 1, 2, and 3 are given in Table 2. For participant N, we have elicited a rule base consisting of 13 fuzzy rules, each of which is expressed by natural language as shown in Table 3.

By observing Table 3, we can find that there exist possibly conflicting rules in the rule base, e.g., the rules #5 and #8 have the same rule premise/antecedent but different consequent ('B' and 'S'), and so do rules #11 and #12 ('VB' and 'B'). Nonetheless, it should be noted that by imitating human-like reasoning fuzzy model also allows for the existence of those seemingly contradictory rules and tolerant of imprecision and/or uncertainty in knowledge or data, which is quite different from conventional knowledge-based (or called expert) systems. From the extracted fuzzy rules, the following personalized knowledge for participant can be discovered:

1) The rules #1 and 2 suggest that the reduced θ band power at EEG-F3 indicates a good operator performance, which was already found in simple tasks in literature (Myung and Pitt, 2009).

2) The rules #3, 6 and 10 suggest that the heightened α band power at EEG-Pz also indicates a good primary task performance of the operator.

3) The rules #4 and 7-9 suggest that the enhanced θ band power at F3 and concomitant reduced α band power at Pz are likely to indicate a poor primary task performance of the operator. For system safety, proper intervention or adjustment measures should be introduced to reassign the tasks between

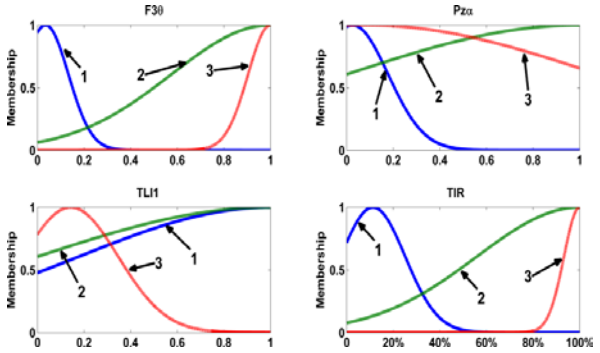

Fig. 4. Gaussian MFs optimized by IPID-PSO.

the operator and automated system. Several literature (Klimesch, 1999; Gevins, Smith, McEvoy and Yu, 1997; Doppelmayr, Finkenzeller and Sauseng, 2008; Boksem, Meijman and Lorist, 2005; Papadelis, Chen, Kourtidou-Papadeli, Bamidis, Chouvarda, Bekiaris and Maglaveras, 2007) showed that under difficult tasks, the θ activity of the operator is often enhanced, accompanied by the reduced α activity. This may imply that the operator performance tends to decline in complex tasks.

All the above findings were made from the individually optimized fuzzy OFS model for participant N. The knowledge may provide some guidelines for the design of adaptive functional allocation based AA system in the future. The extraction of interpretable fuzzy rules (or structured knowledge in the form of If-Then rules expressed with natural language) directly from data is one of essential advantages of fuzzy modeling paradigm, which distinguishes itself clearly from other modeling tools.

5. CONCLUSIONS AND OUTLOOK

In this paper, three inputs, i.e., EEG features, were selected for fuzzy OFS model of each participant. The OFS is quantified by operator performance variable *TIR*, which is

Table 2. Linguistic terms of input/output fuzzy subsets (participant N).

I/O variable	Fuzzy subset		
	1	2	3
F3-θ	Small (S)	Big (B)	Very Big (VB)
Pz-α	Very Small (VS)	Big (B)	Small (S)
TLI	Big (B)	Slightly Big (SB)	Small (S)
TIR	Small (S)	Big (B)	Very Big (VB)

Table 3. Fuzzy rule base optimized by the IPID-PSO algorithm (participant N).

Rule #	Model inputs			Output
	F3-θ	*Pz-α*	*TLI*	*TIR*
1	S	B	S	B
2	S	VS	S	B
3	B	B	B	VB
4	B	S	S	S
5	B	VS	S	B
6	B	B	B	B
7	B	VS	B	S
8	B	VS	S	S
9	VB	VS	S	S
10	VB	B	B	B
11	VB	VS	B	VB
12	VB	VS	B	B
13	VB	S	S	B

treated as the model output. Fuzzy models were constructed to estimate the OFS based on three EEG features. The IPID-PSO algorithm was used to optimize the rule base of individualized fuzzy OFS models. An incremental PID controlled search strategy is endowed with standard PSO algorithm to constitute a new IPID-PSO algorithm, which differs the standard PSO in that it uses a different velocity updating formula, a periodic learning target refreshing mechanism and random mutation. The modelling results demonstrated that fuzzy models optimized by the IPID-PSO algorithm provide an accurate and interpretable estimation of OFS. Some findings were also made based on the analysis of personalized fuzzy rule base identified by the IPID-PSO algorithm. Although the fuzzy modeling paradigm proposed paved the way for accurate OFS estimation, current work can be further improved in the future in the following directions:

1) Data: A randomized, instead of cyclical, manipulation of task load should be considered in the new experimental design. The data from more participants and/or more sessions for a particular participant should be collected to build more accurate fuzzy models.

2) Improvement of IPID-PSO algorithm: Adaptive mutation can be introduced to reduce the randomness of the search and enhance the exploitation ability of the IPID-PSO algorithm.

REFERENCES

Bleil, M. and Manzey, D. (2008). *AutoCAMS 2.0 Manual*, Technical Report, Technical University of Berlin, Germany.

Boksem, M.S., Meijman, T.F. and Lorist, M.M. (2005). Effects of mental fatigue on attention: An ERP study, *Cognitive Brain Research*, vol. **25**(1), pp. 107-116.

Bousefsaf, F., Maaoui, C., Pruski, A. (2013). Continuous wavelet filtering on webcam photoplethysmographic signals to remotely assess the instantaneous heart rate, *BioMed. Signal Proces.*, vol. **8**, pp. 568-574.

Christensen, J., Estepp, J., Wilson, G., and Russell, C. (2012). The effects of day-to-day variability of physiological data on operator functional state classification. *Neuroimage*, vol. **59**, pp. 57-63.

Doppelmayr, M., Finkenzeller, T. and Sauseng, P. (2008). Frontal midline theta in the pre-shot phase of rifle shooting: Differences between experts and novices, *Neuropsychologia*, vol. **46**(5), pp. 1463-1467.

Fairclough, S.H., Venables, L. and Tattersall, A. (2005). The influence of task demand and learning on the psychophysiological response, *Int. J. of Psychophysiology*, vol. **56**(2), pp. 171-184.

Gevins, A., Smith, M.E., McEvoy, L. and Yu, D. (1997). High-resolution EEG mapping of cortical activation related to working memory: effects of task difficulty, type of processing, and practice, *Cerebral Cortex*, vol. **7**(4), pp. 374-385.

Guerrero, F.N., Spinelli, E.M., and Haberman, M.A. (2016). Analysis and simple circuit design of double differential EMG active electrode, *IEEE Trans. on Biomedical Circuits and Systems*, vol. 10(3), pp. 787-795.

Gundel, A. and Wilson, G. (1992). Topographical Changes in the Ongoing EEG Related to the Difficulty of Mental Tasks. *Brain Topogr.*, vol. **5**, pp. 17-25.

Hart, S. (2006). NASA-Task Load Index (NASA-TLX): 20 Years Later, in *Proc. of the Human Factors and Ergonomics Society Annual Meeting*, pp. 904-908.

Klimesch, W. (1999). EEG alpha and theta oscillations reflect cognitive and memory performance: a review and analysis, *Brain Research Reviews*, vol. **29**(2-3), pp. 169-195.

Lin, F., Ko, L., Chuang, C., Su, T., Lin, C. (2012). Generalized EEG-Based Drowsiness Prediction System by Using a Self-Organizing Neural Fuzzy System. *IEEE Trans. on Circuits Syst.*, vol. **59**, pp. 2044-2055.

Lin, F. and Lin, C. *et al.* (2012). Generalized EEG-based drowsiness prediction system by using a self-organizing neural fuzzy system. *IEEE Trans. on Circuits Syst.*, vol. **59**, pp. 2044-2055.

Mehran, K., Giaouris, D., and Zahawi, B. (2010). Stability analysis and control of nonlinear phenomena in boost converters using model-based Takagi–Sugeno fuzzy approach, *IEEE Trans. on Circuits and Systems I: Regular Papers*, vol. 57(1), pp. 200-212.

Myung, J.I. and Pitt, M.A. (2009). Optimal experimental design for model discrimination, *Psychological Review*, vol. **116**(3), pp. 499-518.

Papadelis, C., Chen, Z., Kourtidou-Papadeli, C., Bamidis, P.D., Chouvarda, I., Bekiaris, E. and Maglaveras, N. (2007). Monitoring sleepiness with on-board electrophysiological recordings for preventing sleep-deprived traffic accidents, *Clinical Neurophysiology*, vol. **118**(9), pp. 1906-1922.

Shang, L., Huang, D., Du, J., Zheng, C. (2006). Palmprint recognition using FastICA algorithm and radial basis probabilistic neural network, *Neurocomputing*, vol. **69**, pp. 1782-1786.

Wang, R., Zhang, J., Zhang, Y., and Wang, X. (2012). Assessment of human operator functional state using a novel differential evolution optimization based adaptive fuzzy model. *BioMed. Signal Proces.*, vol. **7**, pp. 490-498.

Wei, Y., Qiu, J., Shi, P., and Chadli, M. (2017). Fixed-order piecewise-affine output feedback controller for fuzzy-affine-model-based nonlinear systems with time-varying delay, *IEEE Trans. on Circuits and Systems I: Regular Papers*, vol. **64**(4), pp. 945-958.

Xiong, W., Yu, W., Lü, J. and Yu, X. (2014). Fuzzy modelling and consensus of nonlinear multiagent systems with variable structure, *IEEE Trans. on Circuits and Systems I: Regular Papers*, vol. **61**(4), pp. 1183-1191.

Zhang, J. and Yang, S. (2014). An incremental-PID-controlled particle swarm optimization algorithm for EEG-data-based estimation of operator functional state. *Biomedical Signal Processing and Control*, vol. **14**, pp. 272-284.

Zhang, J., Yin, Z. and Wang, R. (2015). Recognition of mental workload levels under complex h uman-
machine collaboration by using physiological features an d adaptive support vector machines, *IEEE Trans. on Human-Machine Systems*, vol. **45**(2), pp. 200-214.